16th World Conference on Earthquake, 16WCEE 2017

Santiago Chile, January 9th to 13th 2017

Paper N° 708

Registration Code: S-Q1461044115

SHEAR BEHAVIOR OF UNBONDED PRECAST PRESTRESSED CONCRETE BEAM-COLUMN JOINTS CAUSED VOLUME LOSS IN JOINT PANEL BY SHEATH TUBES

Y. Tajima(1), S. Kishida(2), Z. Tomiyama(3)

(1) *Senior Researcher, Asiss Corporation, tajima@asiss.co.jp*
(2) *Professor, Shibaura Institute of Technology, skishida@sic.shibaura-it.ac.jp*
(3) *Graduate School, Shibaura Institute of Technology*

Abstract

The beam-column joint shear strength (called as V_j) for prestressed concrete (called as P/C) structures is almost depended on a concrete strength in joint panel. Apertures in joint panel are formed by sheath tubes for unbonded precast prestressed concrete (called as unbonded PCaP/C) structures. There are not these apertures for reinforced concrete structures (called as R/C). It is expected that the volume loss with apertures in joint panel causes the decrease of V_j. Conveniently a seismic design expression of the beam-column joint ultimate shear strength for the unbonded PCaP/C structures is applied that of the "Design Guidelines for Earthquake Resistant Reinforced Concrete Buildings Based on Inelastic Displacement Concept" [reference 1]. This guideline is the seismic design provision published by Architectural Institute of Japan (called as AIJ). So the reduction of the beam-column joint ultimate shear strength by apertures formed with sheath tubes isn't considered at present. Therefore, this paper focuses on the effect of joint-panel shear behavior caused volume loss rate (called as R_{vl}) by sheath tubes for unbonded PCaP/C structures. The R_{vl} divided the volume of the apertures formed with a sheath tube by the beam-column joint effective volume. And if the R_{vl} is 0%, it means that there is no aperture in beam-column joint. Previous test results of five specimens in references 2 and 3 were used for cruciform beam-column subassemblages in this paper. The R_{vl} of five specimens were from 0% to 12.1%. All specimens were beam-column joint shear failure.

When the R_{vl} were smaller than 6.1%, the joint shear strengths were larger than lower R/C strength of seismic design provisions by AIJ. On the other hand when the R_{vl} were greater than 6.1%, the tendency of the joint shear strengths was smaller than that. It was obvious that the volume loss by apertures in joint panel causes the decrease of V_j. When the R_{vl} were smaller than 6.1%, the joint-panel area expanded both to the lateral and vertical direction after the peak. On the other hand when the R_{vl} were greater than 6.1%, the joint-panel area expanded to the lateral direction and shrunk to the vertical direction after the peak. From above mention it is found that the beam- column joint panels were failed in the horizontal shear force when the R_{vl} was smaller than 6.1%, and the beam- column joint panels were failed in the vertical (an axial direction) shear force when the R_{vl} was greater than 6.1%. The reduction coefficient considered with apertures in a beam-column joint about the beam-column joint ultimate shear strength is proposed under a simple method in this paper.

The reduction coefficient calculated by a detail method was published in references [2 and 3]. The simple method and the detail method is compared with the seismic R/C design expression. The reduction coefficient proposed the simple method about the beam-column joint ultimate shear strength agreed well with referred test results. And it is an useful expression that the simple method is applied every kind of sheath tube shape.

Keywords: Unbonded Precast Prestressed Concrete, Volume Loss Rate, Joint Shear Strength

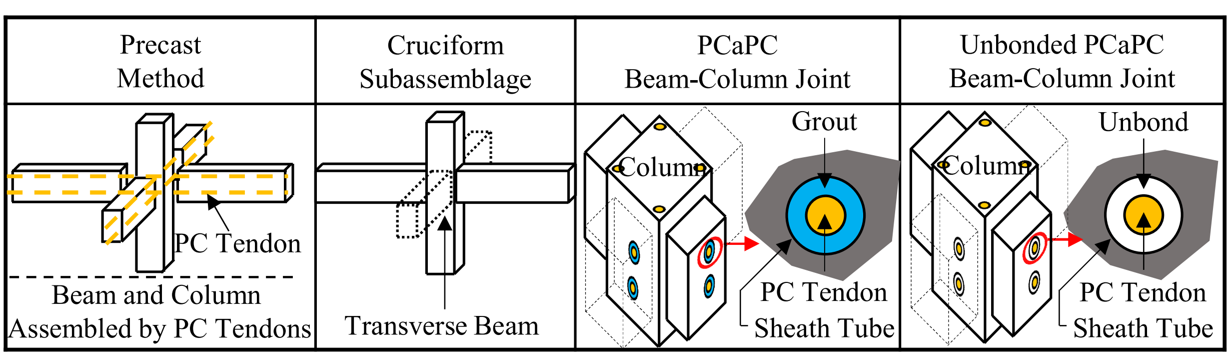

Fig. 1 –Beam-Column Joint

1. Introduction

1.1 Objectives

The V_j for P/C structures is almost depended on a concrete strength in joint panel. Apertures in joint panel are formed by sheath tubes for unbonded PCaP/C structures. There are not these apertures for R/C structures. It is expected that the volume loss with apertures in joint panel causes the decrease of V_j. Conveniently a seismic design expression of the beam-column joint ultimate shear strength for the unbonded PCaP/C structures is applied that of the "Design Guidelines for Earthquake Resistant Reinforced Concrete Buildings Based on Inelastic Displacement Concept" [reference 1]. This guideline is the seismic design provision published by Architectural Institute of Japan (called as AIJ). So the reduction of the beam-column joint ultimate shear strength by apertures formed with sheath tubes isn't considered at present. According to "Guidelines for Structural Design and Construction of Prestressed Concrete Buildings Based on Performance Evaluation Concept (Draft)"[reference 4], it is necessary to estimate the decrease caused by apertures of the ultimate shear strength for the unbonded PCaP/C beam-column joint in designing. The reduction coefficient of the beam-column joint ultimate shear strength by apertures formed with sheath tubes was proposed with the detail method in [reference 3]. But the detail method was complex and unable to be applied to various kinds of sheath shapes. So the joint ultimate shear strength design method considering with apertures for unbonded PCaP/C structures has not been established because of few studies.

Therefore, this paper focuses on the effect of joint-panel shear behavior caused R_{vl} by sheath tubes for unbonded PCaP/C structures using past tests, and is proposed the simple method about the reduction coefficient of the beam-column joint ultimate shear strength by apertures formed with sheath tubes.

In the case of three dimentional PCaP/C beam-column subassemblages, apertures by sheath tubes are formed to two directions (lateral and transverse) in a beam-column joint panel. [see **Fig. 1**]. Such a situation of apertures was applied to the plane specimens in past tests. An effective joint-panel volume is the product of beam depth, column width and joint effective width. In this paper, the volume loss rate R_{vl} is defined as Eq. (1) [see **Fig. 2**]. And if the Rvl is 0%, it means that there is no aperture in beam-column joint.

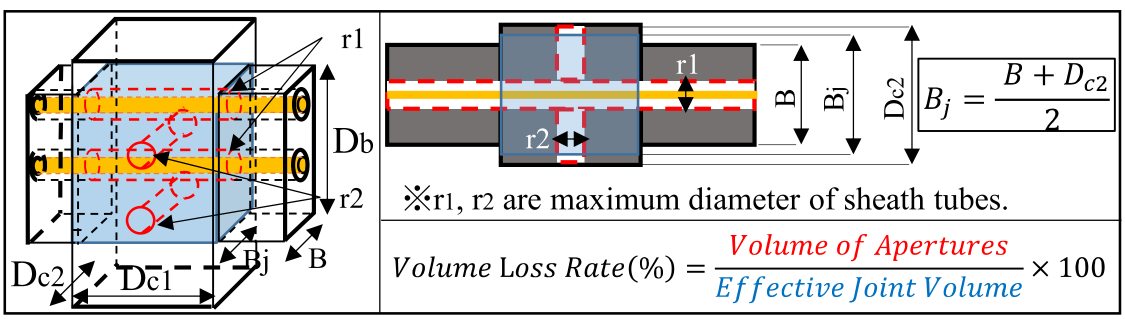

Fig. 2 –Volume Loss Rates

$$R_{vl} = \left\{ \frac{n_1\left(\frac{r_1}{2}\right)^2 \pi D_{c1} + n_2\left(\frac{r_2}{2}\right)^2 \pi D_{c2}}{D_b D_{c1} B_j} \right\} \times 100(\%) \tag{1}$$

Where, r_1 :Diameter of Sheath Tube(mm), r_2 :Diameter of Transverse Sheath Tube(mm), n_1 :Number of Sheath Tube(mm), n_2 :Number of Transverse Sheath Tube (mm), D_{c1}, D_{c2} :Column Width(mm), D_b :Beam Depth(mm) B_j: Joint Effective Width(mm)

2. Previous Test Program

2.1 Specimens

Properties and section dimensions details for specimens are summarized in **Table 1**. Material properties of steel bars and concerte are shown in **Table 2** and **Table 3**. Five cruciform subassemblage specimens with two-fifth scale to actual frames were tested. Beam and column elements were precast separately. Post-tensioning steel bars with deformed surface were used to connect precast R/C beams and column. Beam longitudinal bars were terminated at beam face. Interface mortal with the width of 20mm was set between precast beam and column. The column section was square with 350mm depth. The depth and width of a beam section was 400mm and 250mm, for all specimens. The length from the center of column to the pin-roller support of beam end was 1600mm. The height from the center of beam to the loading point on the top of the column or to bottom support was 1415mm. The shear span ratio were 4.0 in the column and 4.3 in the beam, respectively. Concrete compressive strength of column was 31.3 to 44.4 MPa and that of beam was to 67.1 to 82.7 MPa. Except for Specimen H1 the first post-tensioning force equal to the stress 0.6 times the standard yield strength of the PC tendon was provided. For Spesimen H1 the first post-tensioning force equal to the stress 0.7 times the standard yield strength of the PC tendon was provided.

Specimen H1 was fabricated by PCaP/C method and injected grout mortar into sheath tubes. Other specimens were fabricated by unbonded PCaP/C method. Specimen H1 (R_{vl}=0%) was defined as the standard specimen in this paper. Only Specimen P4 (R_{vl}=4.4%) was arranged symmetrically in the beam section. Sheath tubes of Specimen P6 (R_{vl}=6.1%) were used larger diameter than those of Specimen H1. Transverse apertures by sheath tubes were arranged in joint-panel for Specimen P7 (R_{vl}=12.1%) and P8 (R_{vl}=12.1%) to assume with the unbonded PCaP/C beam-column three-dimensional subassemblages. Though sheath tubes were same volume in the joint-panel both Specimen P7 and P8, two specimens were different arrangements in the joint-panel using different diameter sheath tubes.

2.2 Loading Method and Instrumentation

A loading apparatus is shown in **Fig.3**.The Beam ends were supported by horizontal roller, while the bottom of the column was supported by a universal joint. The reversed lateral horizontal loads and constant axial load in compression (an axial load ratio was 0.13) were applied at the top of the column through a tri-directional joint by three oil jacks, additionally the north-south oil jack was used to prevent the specimens from falling down. In this paper a story drift angle is expressed as a percent ratio of a lateral displacement at the tri-directional joint the column height 2830mm (denoted as R). Specimen H1, P4, P6 were controlled by a story drift angle for one loading cycle of 0.25%, two cycle of 0.5%, 1%, 2%,one cycle 3%, two cycle of 4% respectively, one way loading 5%(Specimen H1, P6), and one way loading 6% (Specimen P4). Specimen P7,P8 were controlled by a story drift angle for one loading cycle of 0.25%, two cycle of 0.5%, 1%, 1.5%, 2%, one cycle 3%(Specimen P7), two cycle 3% (Specimen P8), two cycle of 4% respectively. Lateral forces, column axial load and beam shear forces were measured by load-cells. Story drift, beam and column deflections, and local displacement of a joint panel were measured by displacement transducers. Strains of prestressing steel bars, beam bars, column bars and joint lateral reinforcement were measured by strain gauges. Concrete normal strain at a beam end adjacent to a column face was measured by strain gauges attached on concrete surface.

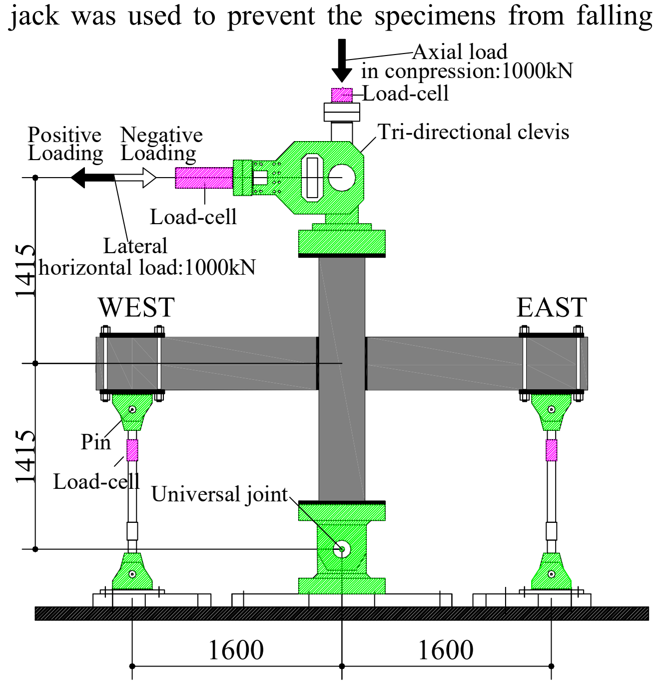

Fig. 3 – Loading Apparatus

Table 1 –Properties of Specimens

Specimens	H1	P4	P6	P7	P8
Type	PCaPC	Unbonded PCaPC			
Volume Loss Rates	0%	4.4%	6.1%	12.1%	
Grout	74.6N/mm^2	None			
Diameter of Sheath Tubes	2-φ1052	2-φ1055	2-φ1065	2-φ1065	2-φ1065
Transeverse Sheath Tubes	None			2-φ1065	4-φ1048
PC Tendons	2-36mm				
	SBPD930/1080	SBPR1080/1230	SBPD1080/1230		SBPR1080/1230
First Prestressing Stress /Yeild Strength	0.7	0.6			
Column Longitudinal Bar	12-D25	4-D32	12-D25		
	SD490	SBPR930/1080	SD490		
Joint Lateral Reinforcement	D10				
	KSS785@90	SD345@100	KSS785@90		
Common Factor	Axial Load Ratio	:0.13	Beam Stiirrup	:D10(SD345)@100	
	Beam Section	:250mm×400mm	Beam Erection Bar	:4-D13(SD345)	
	Column Section	:350mm×350mm	Column Hoop 1	:D10(SD345)@90(H1/P6)	
	Interface Mortal	:20mm	Column Hoop 2	:D10(SD345)@100(P4/P7/P8)	
Shape of Specimens and Beam Section	Column Section and Detail of Beam-Column joint				

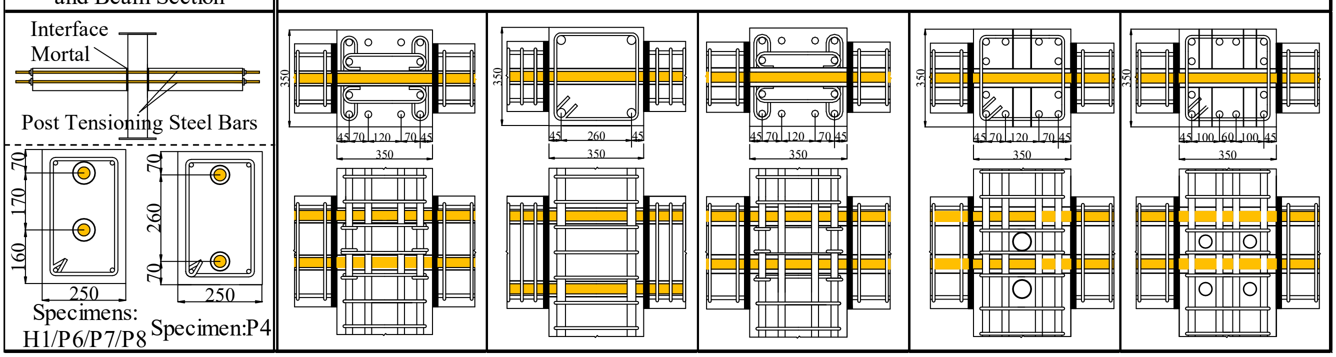

Table 2 – Material Properties of steel bars

Specimens	H1			P4			P6			P7			P8		
Steel Bars	σ_y	E_s	ε_y	σ_y	E_s	ε_y	σ_y	E_s	ε_y	σ_y	E_s	ε_y	σ_y	E_s	ε_y
	N/mm^2	kN/mm^2	μ	N/mm^2	kN/mm^2	μ	N/mm^2	kN/mm^2	μ	N/mm^2	kN/mm^2	μ	N/mm^2	kN/mm^2	μ
Column Longitudinal Bar	508	185	2754	1011	191	7880	538	188	2870	542	196	2902	551	192	2919
Column Hoop	372	179	2105	395	171	2470	364	176	2208	371	187	2425	370	179	2278
Joint Lateral Reinforcement	1010*	181	7579				942*	175	7372	1009*	196	7143	914*	177	7166
Beam Longitudinal Bar	369	169	2037	385	186	2134	352	170	2364	379	193	2020	The same value of Specimen P7		
Beam PC tendon	1143*	208	7490	1155*	198	8500	1169*	211	7534	1119*	203	7515	1152*	201	7726

σ_y: Yeild Strength, E_s: Young's Modulus, ε_y: Yeild Strain, *:Yeild strain determinated nominally by 2000μ offset method

Table 3 – Material Properties of concrete

(a) Concrete of Column

	Unit	H1	P4	P6	P7	P8
Compressive Strengh	N/mm^2	44.4	31.8	32.1	31.3	36.9
Secant Modules	kN/mm^2	32.4	25.0	27.8	25.3	26.1
Strain at Maximum Strength	μ	2153	2331	1895	1686	2471
Tensile Strength	N/mm^2	2.7	2.3	2.8	2.2	3.2

(b) Concrete of Beam

	Unit	H1	P4	P6	P7/P8
Compressive Strengh	N/mm^2	82.7	76.9	67.1	81.3
Secant Modules	kN/mm^2	41.7	34.9	36.9	38.9
Strain at Maximum Strength	μ	2875	2936	2417	2518
Tensile Strength	N/mm^2	4.1	4.4	3.9	3.3

3. Test Results

3.1 Crack Pattern and Failure Mode

Crack patterns at the maximum story shear force and the story drift angle of 4% are shown in **Table 4**. Flexural cracks in beam and column and diagonal shear cracks in joint panel were observed for all specimen. Additionally numbered flexural cracks in beam of Specimens H1 were greater than other unbonded PCaP/C specimens. After the maximum story shear force, post-tensioning steel bars passing through beams locally yielded for Specimen H1 and the column longitudinal bars locally yielded for Specimen H1 and P8. The joint lateral reinforcement for Specimen P4 yielded at the story drift angle of 0.9% and it for Specimen P6, P7, P8 yielded at the story drift angle 3-6%. After diagonal shear cracks in a joint panel extended as the increase in the story drift angle, the shell concrete spalled off. Joint shear failure occurred for all specimens. Though the main direction of the joint shear force to a failure was different in each specimen, that is described in detail later[**4.3**].

Table 4 – Crack pattern

Specimens	H1	P4	P6	P7	P8
R_{vl}(%)	0	4.4	6.1	12.1	12.1
At Maximum Story Shear Force	 R=2%	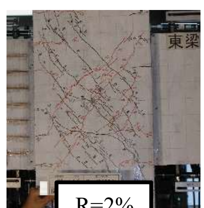 R=2%	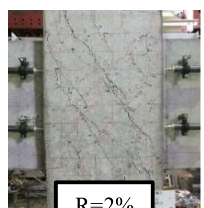 R=2%	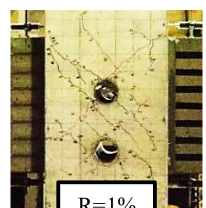 R=1%	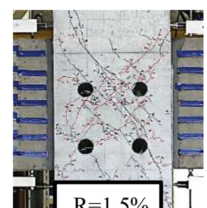 R=1.5%
At The Story Drift Angle of 4%	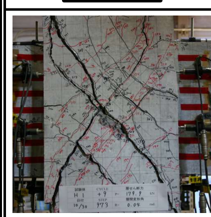				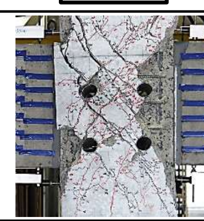

3.2 Story Shear Force– Drift Relations

The story shear force – story drift angle relations are shown in **Fig.4**. The story shear force was computed from moment equivalent between beam shear force and the horizontal force at the loading point on the top of the column. The occurrence of flexural cracking in column, diagonal shear cracking in a joint panel and maximum story shear, and yielding of each bars that was judged from output of strain gauges on them are marked. For all specimens exhibited origin-oriented loops at first, and gradually showed spindle-shaped hysteresis loops as the increase in story drift and resembled hysteresis characteristic of R/C assemblage. Specimen H1, P4, P6 which are PCaP/C and unbonded PCaP/C reached maximum story shear force in the story drift angle of 2%. On the other hand, Specimen P7, P8 which are unbonded PCaP/C with transeverse apertures reached maximum story shear force in the small story drift angle . Former reached maximum story shear force at R=1%, latter reached at R=1.5%. It was found that deformation performance of Specimens with apertures were smaller than specimens without apertures.

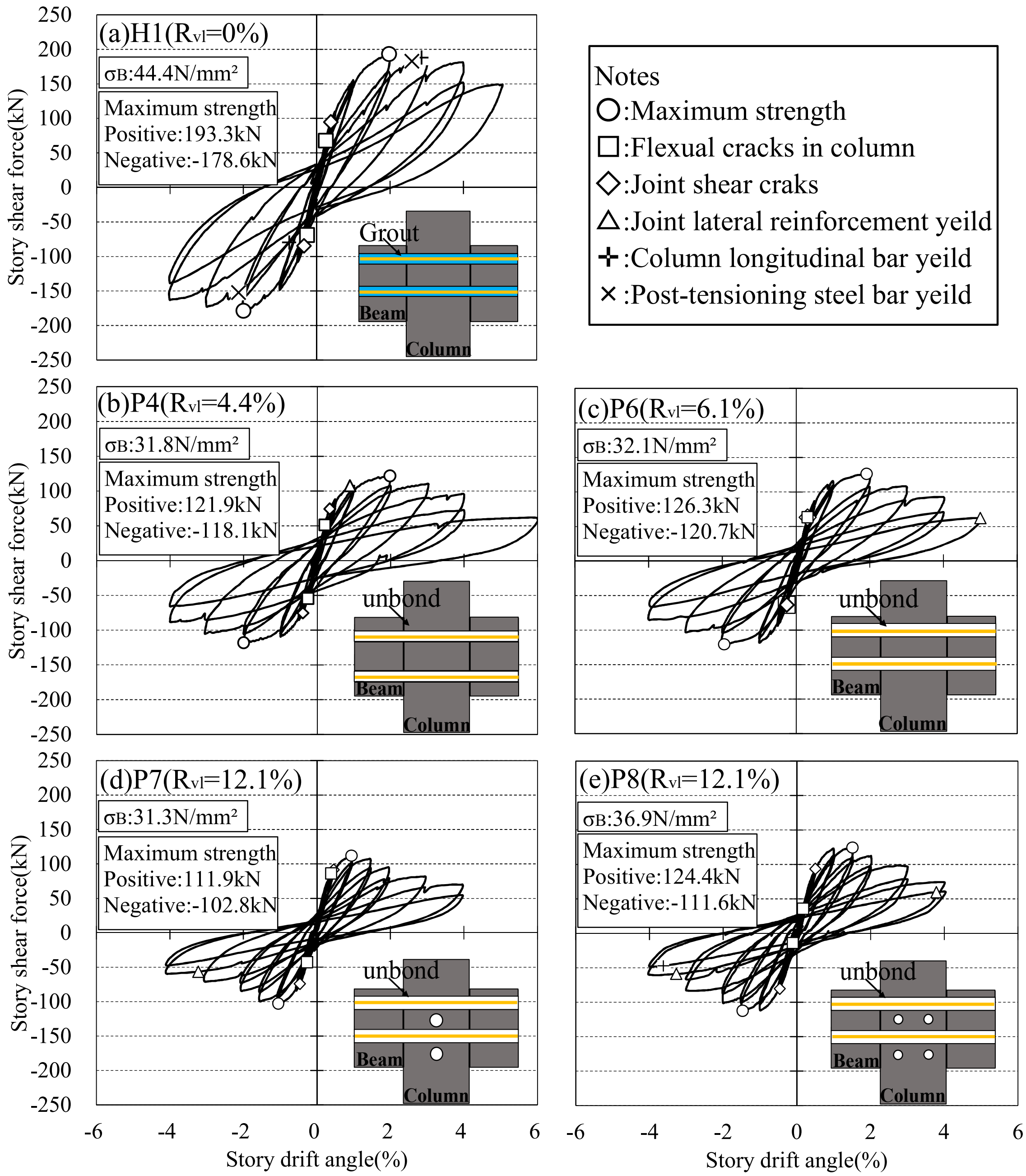

Fig. 4 – Relations between story shear and story drift

4. Discussions about Test Results

4.1 Normalized Story Shear Force– Story Drift Relations

The envelope curves of normalized story shear force – story drift relations are shown in **Fig.5**. **Fig.5** (a) is shown envelope curves of PCaP/C and unbonded PCaP/C. **Fig.5** (b) is shown unbonded PCaP/C with transeverse apertures. Envelope curve of Specimen P6 is also shown as a reference value in **Fig.5 (b)**. The normalized story shear force decreased as the R_{vl} increased. Normalized story shear force is defined as Eq. (2).

$$\text{Normalized Story shear Force} = \frac{\textit{Story Shear Force}}{\sigma_B D_{c1} B_j} \tag{2}$$

Where, σ_B: Compressive Strength of Column Concrete(N/mm^2) D_{c1},:Column Width(mm), B_j: Joint Effective Width(mm)

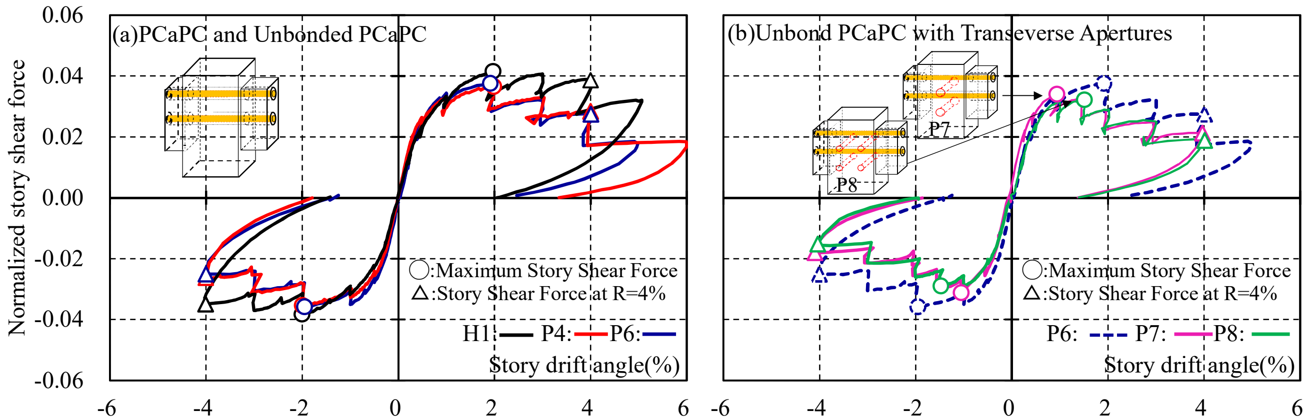

Fig.5 –Envelope Curves of Normalized Story Shear Force

The ratio of respective maximum story shear forces to standard value-volume loss rates relations are shown in **Fig.6**. The ratio of respective maximum story shear force to standard value of **Fig.6(a)** is defined as Eq. (3) and that of **Fig.6 (b)** is defined as Eq. (4).

$$\text{Ratio in } \textbf{Fig.6(a)} \ (\%) = \frac{Normalized\ \ Maximum\ \ Story\ \ Shear\ Force\ \ of\ Respective\ \ Specimens}{Normalized\ \ Maximum\ \ Story\ \ Shear\ Force\ \ of\ \ Specimen\ \ H1} \times 100 \tag{3}$$

$$\text{Ratio in } \textbf{Fig.6(b)} \ (\%) = \frac{Normalized\ \ Story\ \ Shear\ Force\ \ at\ R=4\%\ of\ respective\ \ Specimens}{Normal\ ized\ Maximum\ \ Story\ \ Shear\ Force\ \ of\ respective\ \ Specimens} \times 100 \tag{4}$$

In **Fig.6(a)**, maximum story shear forces for Specimen (P4 and P6) were 10% as small as standard value Specimen H1 and Specimen (P7 and P8) were 15-20% as small as standard value. In **Fig.6(b)**, all specimens at R=4% were 10%-55% as small as respective maximum story shear force. As the volume loss rate R_{vl} increased, the tendency of respective rates decreased.

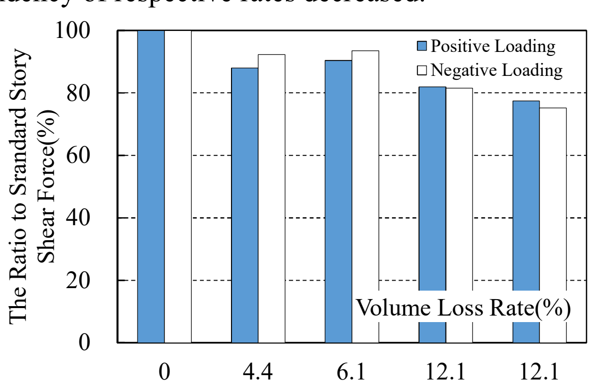

Fig.6 (a)– The Ratio of Respective Maximum Story Shear Forces to Standard Value-Volume Loss Rates Relations (At Maximum Story Shear Force)

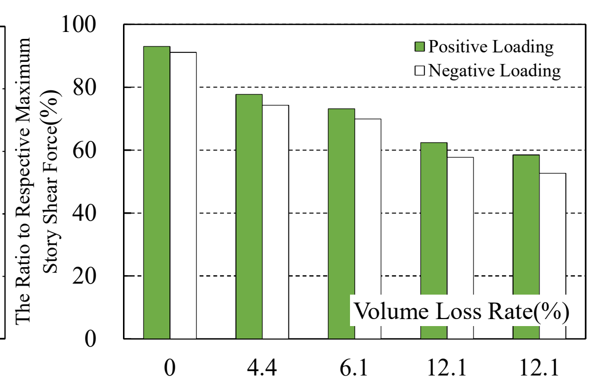

Fig.6 (b)– The Ratio to Respective Maximum Shear Forces-Volume Loss Rates Relations (At Story Drift Angle 4%)

4.2 Deformation in Joint-Panel

The instrumentation for joint-panel deformation is shown in **Photo 1**. Drawing method of deformtion in joint-panel is shown in **Fig. 9**. Displacements measured by two horizontal and vertical displacement transducers from the story drift angle of 1% to 4% were distributed equally to quadrangle which was composed one – fiftieth side. The lateral and vertical displacements in a joint panel are shown in **Fig.10**. Deformation of Specimen H1 was drawed as black dotted line in **Fig.10**. The lateral and vertical average strains in joint panel are shown in **Fig.11(a)** and **(b)**, respectively. In **Fig.10**, **Fig.11**, the joint panels for Specimen H1 and P4 expanded to the lateral and vertical direction. On the other hands when R_{vl} was greater than 6.1%, the joint panels expanded only to the lateral direction.

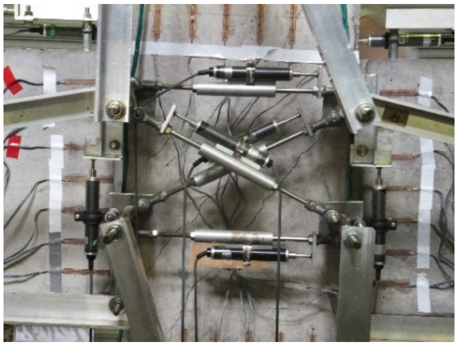

Photo1 – Instrumentation for Joint Panel

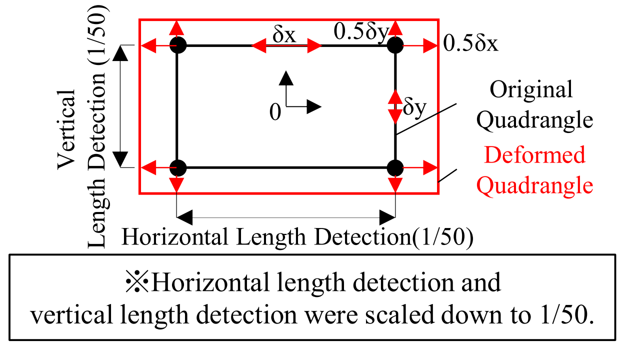

Fig.9 – Drawing Method in Joint-Panel

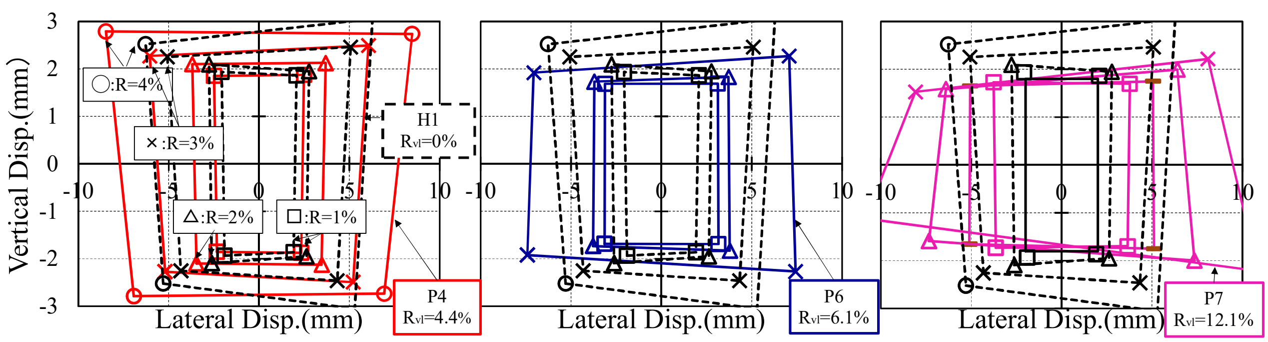

(a) Specimen P4 and H1 (b) Specimen P6 and H1 (c) Specimen P7 and H1

Fig.10 – Vertical Displacement-Lateral Displacement relations in Joint-Panel

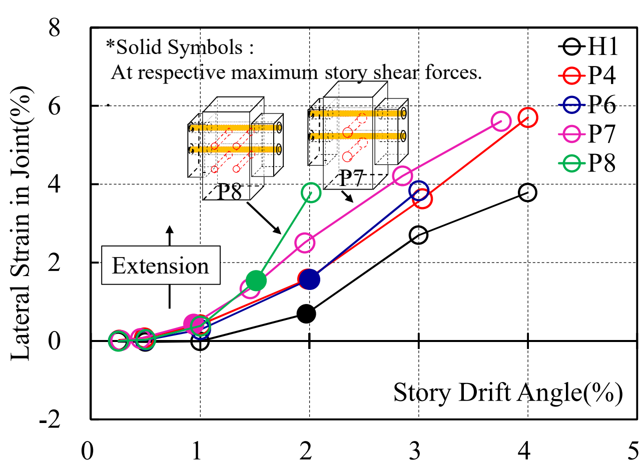

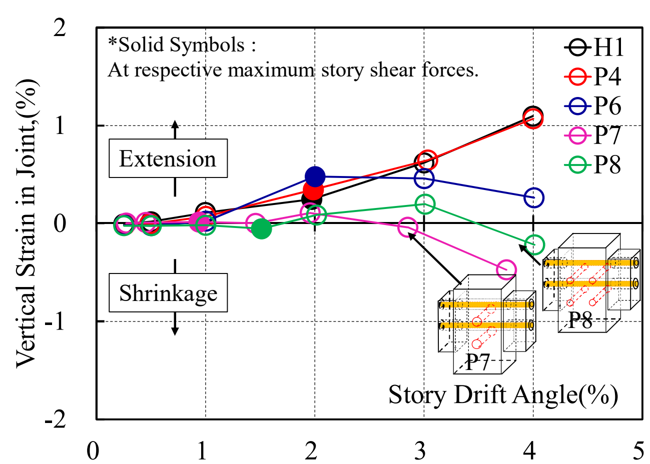

Fig.11(a) – Average Lateral Strain in Joint-Panel **Fig.11(b)** – Average Vertical Strain in Joint-Panel

4.3 Failure Direction for Specimen P7 and P8

Envelope curves of the relations between normalized joint input shear force are shown in **Fig.12**. Joint input shear force were caluculated by Reference[1](see **Fig.13**). Joint input shear force in each direction are normalized strengths of R/C beam-column joints calculated by seismic design provisions by Architectual Institute of Japan[1]. In **Fig.12(a)** and **(b)** normalized horizontal joint input shear force is called as V_{jh}. In **Fig.12(c)** vertical normalized joint input shear force is called as V_{jv}. In **Fig.12(a)** it was found that V_{jh} for Specimen H1, P4 and P6 were reached the peak at a story drift angle of 2%. In **Fig.12**(b) it was found that story drift angles at the times of the maximum story shear force and the maximum V_{jh} weren't the same story drift angle for Specimen P7 and P8. Therefore, the V_{jv} was calculated for Specimen P7 and P8(see **Fig.13**).

As a result of that calculation, story drift angles at the times of the maximum story shear force and the maximum V_{jh} were the same story drift angle for Specimen P7 and P8 in **Fig.12**(c). As mentioned above, it was obvious that the main direction of the joint shear force to a failure was a vertical (axial) direction for Specimen P7 and P8. The reason why shear failure to a vertical direction was occurred is that the vertical minimum section of joint was smaller than the horizontal minimum section of joint (see **Fig.14 and 15**). It was thought that a boundary of whether a direction of a joint shear failure was horizontal or vertical existed between (R_{vl}=6.1%) and (R_{vl}=12.1%) in **Fig.15**.

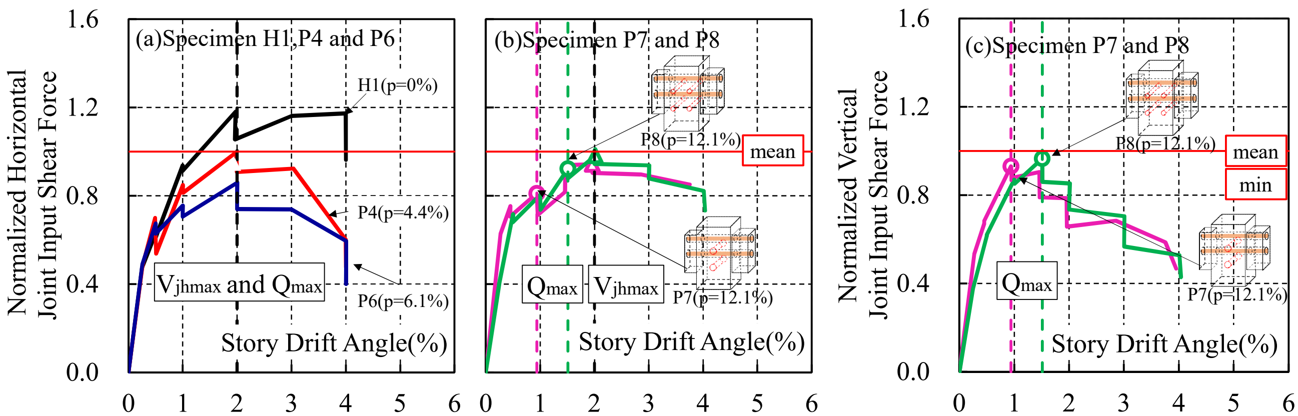

Fig.12 –Normalized Joint Input Shear Force-Story Drift Angle Relations

Horizontal Joint Input Shear Force		Vertical Joint Input Shear Force	
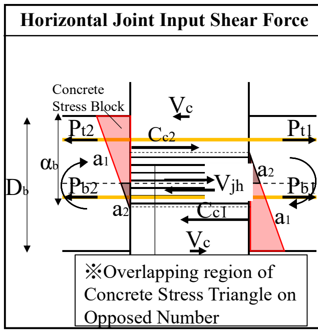	$V_{jh} = P_{t1} - P_{t2} + \alpha_1 C_{c2} - \alpha_2 C_{c1} - V_c$ $C_{c1} = P_{t1} + P_{b1}, C_{c2} = P_{t2} + P_{b2}$ $\alpha_1 + \alpha_2 = 1$ $\underline{D_b/2 \geq \alpha_b}$ $\alpha_2 = 0$ $\underline{D_b > \alpha_b > D_b/2}$ $\alpha_2 = \frac{(\alpha_b - D_b/2)^2}{{\alpha_b}^2}$ $\underline{\alpha_b \geq D_b}$ $\alpha_2 = \frac{(\alpha_b - D_b/2)^2 - (\alpha_b - D_b)^2}{{\alpha_b}^2}$	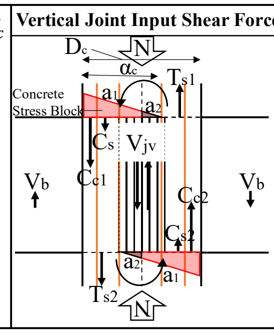	$V_{jv} = T_{s2} + C_{s1} + \alpha_1 C_{c1} - \alpha_2 C_{c2} - V_b$ $C_{c1} = N + T_{s1} - C_{s1}$ $\alpha_1 + \alpha_2 = 1$ $\underline{D_c/2 \geq \alpha_c}$ $\alpha_2 = 0$ $\underline{D_c > \alpha_c > D_c/2}$ $\alpha_2 = \frac{(\alpha_c - D_c/2)^2}{{\alpha_c}^2}$ $\underline{\alpha_c \geq D_c}$ $\alpha_2 = \frac{(\alpha_c - D_c/2)^2 - (\alpha_c - D_c)^2}{{\alpha_c}^2}$

Fig.13 – Caluculation Method of Joint Input Shear Force

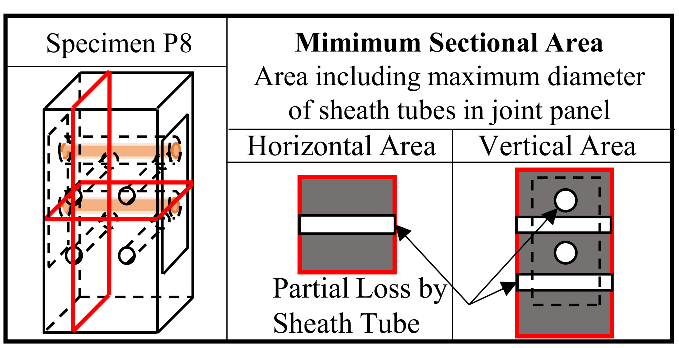

Fig.14 – Difinition of Minimum Section Area

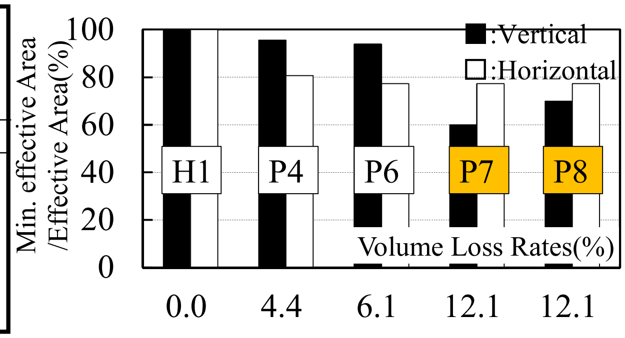

Fig.15–Minimum Section of Joint Area

4.4 Proposal Resistance Area against Input Shear Force

Proposed resistance beam-column joint area against input shear force is called as $_{vr}A$ in this paper. The simple method is proposed in this paper and the detail method is quoted from [reference 2 and 3]. Simple method of estimation for resistance area is shown in **Fig.16** and defined as Eq. (5) and (6). Detail method of estimation for resistance area is shown in **Fig.17** and defined as Eq. (7) and (8). Simple method is easy and applicable in every kind of sheath tube shapes. On the other hand detail method is complex, but it can be expressed precisely. Deep examination is described to the next chapter.

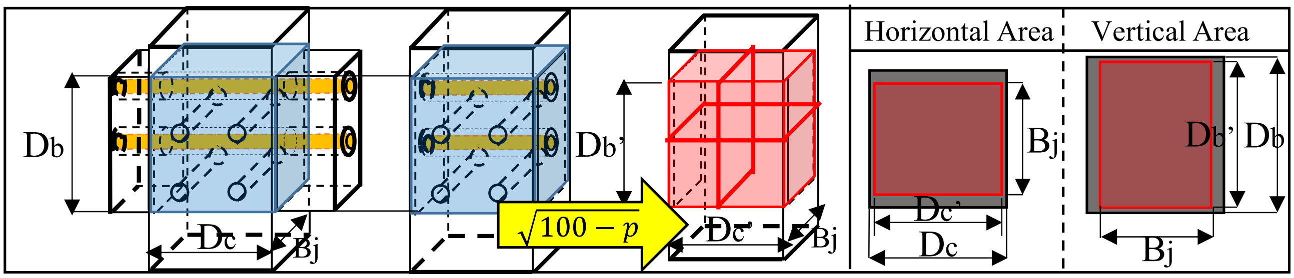

Fig.16 – Simple Method of Estimation for resistance area

$$\text{Horizontal } {}_{vr}A = \frac{1}{10} B_j D_c \sqrt{(100 - R_{vl})} \tag{5}$$

$$\text{Vertical } {}_{vr}A = \frac{1}{10} B_j D_b \sqrt{(100 - R_{vl})} \tag{6}$$

Where B_j: Joint Effective Width, D_c: Column Width, D_b: Beam Depth, R_{vl}: Volume Loss Rates

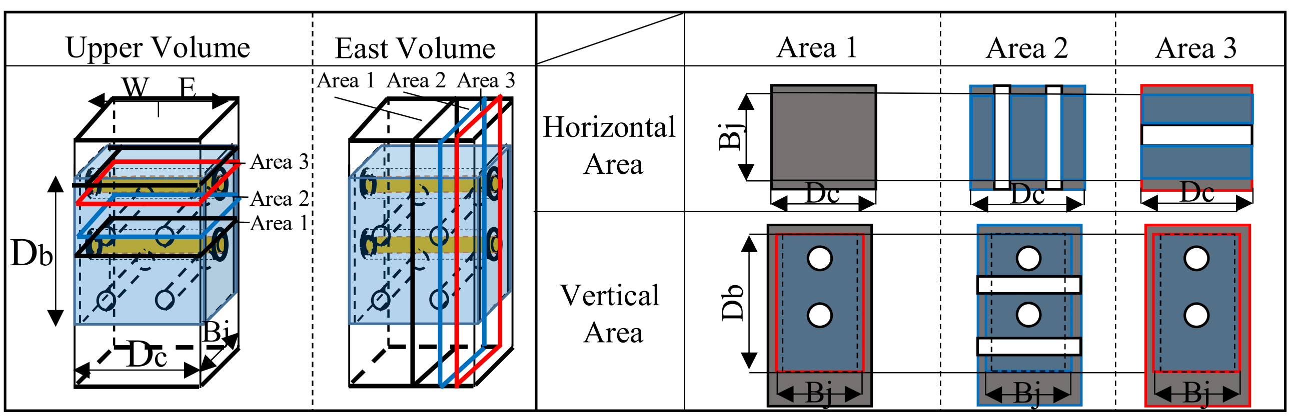

Fig.17 – Detail Method of estimation for resistance area

(i) Section area at center location of beam-column joint is calculated.

(ii) In upper and east half volume, section area (a blue range) including outside diameter of respective sheath tubes which are arranged in east-west and south-north direction and solidity concrete sectional area are calculated.

(iii) In downer and west half volume half, section area are calculated in the same way.

(iv) Total section area is divided by number of sections.

$$\text{Horizontal } {}_{vr}A = \frac{Total\ Section\ Area}{Number\ of\ sections} = \frac{3 \times Area1 + 2 \times Area2 + 2 \times Area3}{3 + 2 + 2} \tag{7}$$

$$\text{Vertical } {}_{vr}A = \frac{Total\ Section\ Area}{Number\ of\ sections} = \frac{3 \times Area1 + 2 \times Area2}{3 + 2} \tag{8}$$

4.5 Investigation of Proposed Method for Joint Input Shear Force

Normalized horizontal joint input shear force at maximum story shear force-volume loss rate relations are shown in **Fig. 18**. **Fig. 18**(a) indicates the ratios of design estimation for the AIJ provision to the test results. **Fig. 18**(b) indicates the ratios of design estimation for the simple method to the test results. And **Fig. 18**(c) indicates the ratios of design estimation for the detail method to the test results. Red lines are average strengths predicted by the AIJ provision in **Fig. 18**. In other words, it was meant that design method was agreed well with test results if the plotted point was close to 1.0. It was obvious that the design estimation ignored apertures in joint panel for the AIJ provision was not agreed well with test results as the volume loss rates increased in **Fig. 18**(a). On the other hand, the design estimations considered apertures in joint panel for the simple and detail methods were improved as the volume loss rates increased in **Fig. 18**(b) and (c). Normalized vertical joint input shear force at maximum story shear force-volume loss rates relations are shown in **Fig. 19**. **Fig. 19** was focused on Specimen P7 and P8. The tendency of improvement in **Fig. 19** was similar to that in **Fig. 18**. It was showed that simple and detail methods, which were predicted horizontal and vertical ultimate joint shear strength considered with lateral and transverse apertures in joint panel, were capable of a better precision than the seismic R/C design expression.

The detail method is complex but the simple method is brief. So the simple method is the useful expression because it is easily applied every kind of sheath tube shapes.

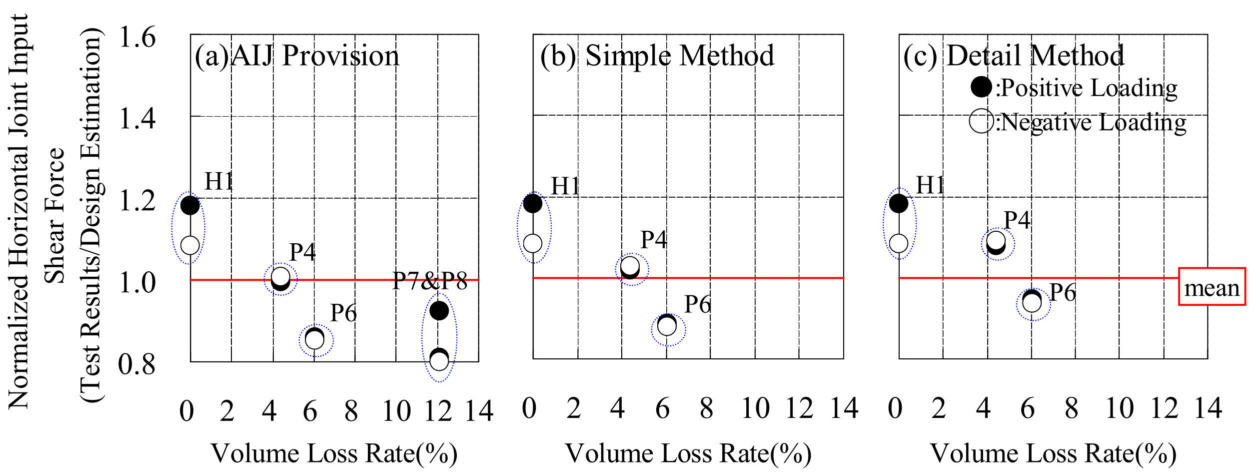

Fig.18 – Normalized Horizontal Joint Input Shear Force at Maximum Story Shear Force-Volume Loss Rate Relations

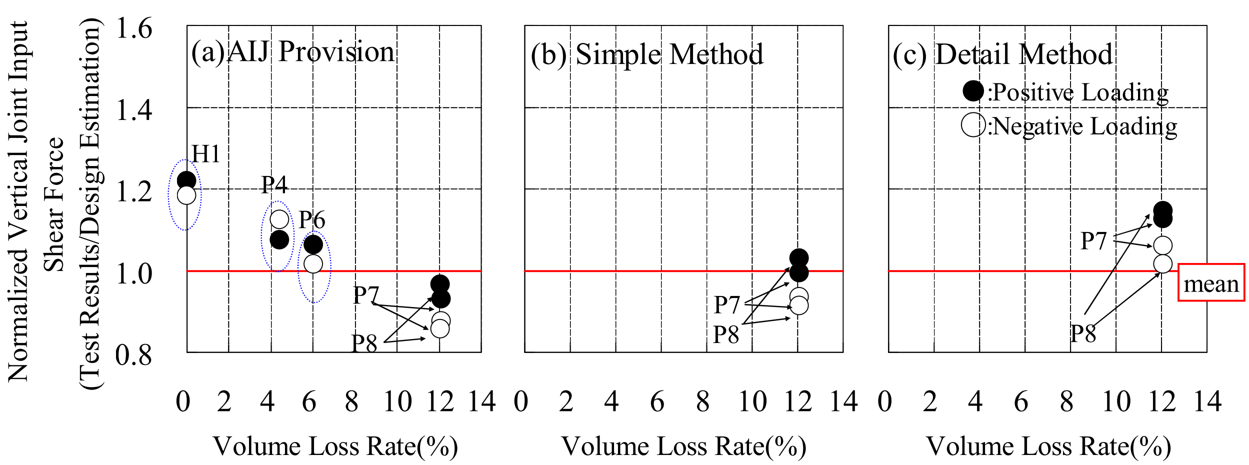

Fig.19 – Normalized Vertical Joint Input Shear Force at Maximum Story Shear Force-Volume Loss Rate Relations

5. Conclusions

The following conclusions can be drawn from the present study:

(1) Deformation performance of Specimen P7 and P8 in joint-panel were smaller than Specimen H1, P4 and P6. Joint shear strength for unbonded PCaP/C structures decreased as the R_{vl} increased in past test results. Reductions of story shear forces from the maximum to story drift angle of 4% were tended to decrease as the increase in the R_{vl}.

(2) Beam-column joint panel deformations were changed when the R_{vl} became greater than 6.1%. Especially beam-column joint panels for Specimen P7 and P8 were expanded only to the lateral direction as the story drift angles were large. Specimen P7 and P8 with transverse apertures in joint-panel failed in vertical shear.

(3) The simple method of joint shear strength for unbonded PCaP/C structures was proposed in this paper. It was showed that simple and detail methods, which were predicted horizontal and vertical ultimate joint shear strength considered with lateral and transverse apertures in joint panel, were capable of a better precision than the seismic R/C design expression. The detail method is complex but the simple method is brief. So the simple method is the useful expression because it is easily applied every kind of sheath tube shapes.

References

[1] Architectural Institute of Japan, Design Guidelines for Earthquake Resistant Reinforced Concrete Buildings Based on Inelastic Displacement Concept, 1999.

[2] Y. Tajima, S. Kishida, Z. Tomiyama. (2015). Effect of Volume Loss Rate to Sheath Tubes in the Unbonded Precast Prestressed Concrete Frame Assembled by Post Tensioning Steel Bars. Summaries of Technical Papers of Annual Convention of Japan Concrete Institute. DVD-Rom,319-324

[3] Z. Tomiyama, K. Yamashita, S. Kishida, Y. Tajima. (2015). Effect of Vacant Space to Sheath Tubes to Maximum Story Shear and Shear Strength of Beam-Column Joint in the Unbonded Precast Prestressed Concrete Frame Assembled by Post Tensioning Steel Bars (Part2 Investigation of Shear Strength of Beam-Column Joint). Summaries of Technical Papers of Annual Meeting of Architectural Institute of Japan. DVD-Rom,717-718

[4] Architectural Institute of Japan, Guidelines for Structural Design and Construction of Prestressed Concrete Buildings Based on Performance Evaluation Concept (Draft), 2015.